INTEGR. COMP. BIOL., 43:591–602 (2003)

A Fourier Tool for the Analysis of Coherent Light Scattering by Bio-Optical Nanostructures[1]

RICHARD O. PRUM*[2] AND RODOLFO H. TORRES†[3]

*Department of Ecology and Evolutionary Biology, and Natural History Museum, University of Kansas, Lawrence, Kansas 66045-7561

†Department of Mathematics, University of Kansas, Lawrence, Kansas 66045-7561

SYNOPSIS. The fundamental dichotomy between incoherent (phase independent) and coherent (phase dependent) light scattering provides the best criterion for a classification of biological structural color production mechanisms. Incoherent scattering includes Rayleigh, Tyndall, and Mie scattering. Coherent scattering encompasses interference, reinforcement, thin-film reflection, and diffraction. There are three main classes of coherently scattering nanostructures—laminar, crystal-like, and quasi-ordered. Laminar and crystal-like nanostructures commonly produce iridescence, which is absent or less conspicuous in quasi-ordered nanostructures. Laminar and crystal-like arrays have been analyzed with methods from thin-film optics and Bragg's Law, respectively, but no traditional methods were available for the analysis of color production by quasi-ordered arrays. We have developed a tool using two-dimensional (2D) Fourier analysis of transmission electron micrographs (TEMs) that analyzes the spatial variation in refractive index (available from the authors). This Fourier tool can examine whether light scatterers are spatially independent, and test whether light scattering can be characterized as predominantly incoherent or coherent. The tool also provides a coherent scattering prediction of the back scattering reflectance spectrum of a biological nanostructure. Our applications of the Fourier tool have falsified the century old hypothesis that the non-iridescent structural colors of avian feather barbs and skin are produced by incoherent Rayleigh or Tyndall scattering. 2D Fourier analysis of these quasi-ordered arrays in bird feathers and skin demonstrate that these non-iridescent colors are produced by coherent scattering. No other previous examples of biological structural color production by incoherent scattering have been tested critically with either analysis of scatterer spatial independence or spectrophotometry. The Fourier tool is applied here for the first time to coherent scattering by a laminar array from iridescent bird feather barbules (*Nectarinia*) to demonstrate the efficacy of the technique on thin films. Unlike previous physical methods, the Fourier tool provides a single method for the analysis of coherent scattering by a diversity of nanostructural classes. This advance will facilitate the study of the evolution of nanostructural classes from one another and the evolution of nanostructure itself. The article concludes with comments on the emerging role of photonics in research on biological structural colors, and the future directions in development of the tool.

INTRODUCTION

The colors of organisms are created by chemical interactions with molecular pigments and by optical interactions of incident light with biological nanostructures. The latter class, called structural colors, form an important component of the phenotype of many animals (Fox, 1976; Nassau, 1983; Herring, 1994; Parker, 1999; Srinivasarao, 1999) and even some plants. (Lee, 1991, 1997). An understanding of the evolution of structural colors and their functions in the lives of organisms will require a thorough appreciation of the physical mechanisms of structural color production and the development of the biological nanostructures that produce them.

The anatomical structures that produce biological structural colors are strikingly diverse (Fox, 1976; Nassau, 1983; Herring, 1994; Parker, 1999; Srinivasarao, 1999). This anatomical diversity has fostered a diversity of proposed physical explanations. In many instances, the physical explanations emphasize anatomical features rather than genuine differences in physical mechanisms. Consequently, there may be several redundant methods to describe mechanisms of color production by an anatomical system, and different numerical tools have been proposed for analyzing color production by different anatomical systems that share a common physical mechanism. This traditional framework has created several intellectual limitations. First, it has prevented a unified physical and mechanistic synthesis of the anatomical diversity. Second, the study of the evolution of color producing nanostructures has been limited by the mathematical incompatibility of the physical tools for analyzing structural color production by different classes of nanostructure. Since the analytical tools for studying different structures are incompatible, it has been impossible to study the evolution of color production *among* these nanostructural or anatomical classes.

One of the primary goals of this paper is to present an alternative classification of mechanisms of biological color production, which emphasizes a single fundamental physical distinction—incoherent *vs.* coherent light scattering. The second goal is to describe a new tool we have been developing that applies Fourier

[1] From the Symposium *Comparative and Integrative Vision Research* presented at the Annual Meeting of the Society for Integrative and Comparative Biology, 4–8 January 2003, at Toronto, Canada.

[2] Current address: Department of Ecology and Evolutionary Biology, Yale University, P.O. Box 208105, New Haven, CT 06520; e-mail: richard.prum@yale.edu

[3] E-mail: torres@math.ku.edu

analysis to the study of biological structural color production by coherent scattering. A major advantage of this tool is that it will analyze color production by all major classes of coherently scattering materials.

INCOHERENT *VS.* COHERENT SCATTERING

Despite the diversity of proposed mechanisms of structural color production (Fox, 1976; Herring, 1994; Parker, 1999; Srinivasarao, 1999), most mechanisms of color production can be well understood as variations of light scattering. As light is propagated through a biological medium, components of that light are either propagated forward in the medium, absorbed by molecules, or scattered in all directions within the medium. The component of scattered light can increase dramatically as light travels from a medium of one refractive index to another. Most biological structural colors are produced by light scattering from nanometer scale variation in refractive index.

Mechanisms of biological color production can be classified according to a fundamental physical dichotomy as either incoherent or coherent scattering (van de Hulst, 1981; Bohren and Huffman, 1983). Incoherent and coherent scattering differ in whether the behavior of scattered light is independent of or dependent upon the phases of scattered light waves, and in whether the phases of scattered wave can be ignored or must be taken into account to describe the behavior of scattered light waves.

Incoherent scattering occurs when individual light scattering objects are responsible for differentially scattering visible wavelengths (Fig. 1A). Incoherent scattering models assume that light scattering objects within a medium are spatially independent, that is that they are randomly distributed in space at the scale of visible wavelengths. If the scatterers themselves are randomly distributed in space over distances of the same order of magnitude as the wavelengths of visible light, the phase relationships among the scattered waves are also random, and can be ignored in any description of light scattering behavior of the medium. Consequently, incoherent scattering models ignore the phase relationships among the scattered waves, and describe color production as the result solely of differential scattering of wavelengths by the individual scatterers themselves (van de Hulst, 1981; Bohren and Huffman, 1983).

In contrast, coherent scattering occurs when the spatial distribution of light scatterers is not random with respect to the wavelengths of visible light, so that the phases of scattered waves are also non-random (Bohren and Huffman, 1983). Consequently, coherent scattering models describe color production in terms of the phase interactions among light waves scattered by multiple scatterers (Fig. 1B). Light waves scattered by independent objects that are out of phase will destructively interfere with one another and cancel out, whereas scattered waves that are in phase with one another will constructively reinforce each other and will be *coherently scattered* by the material. The phase relationships among the wavelengths scattered by two objects are given by the differences between the path lengths of the waves scattered by the two objects and the average refractive index of the medium.

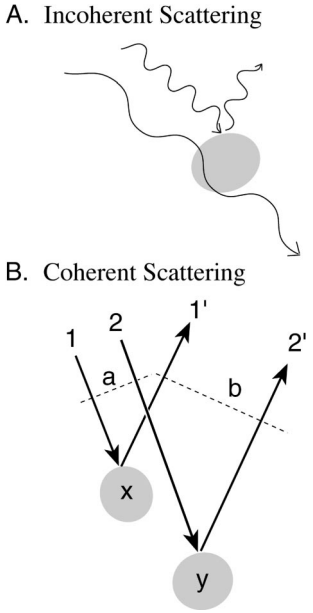

FIG. 1. Comparison of incoherent and coherent scattering mechanisms of biological structural color production. (A) Incoherent scattering is differential scattering of wavelengths by individual light scattering objects. Incoherent scattering by small particles (*i.e.,* Rayleigh or Tyndall scattering) preferentially scatters smaller wavelengths. The phases relationships among light waves scattered from different objects are random. (B) Coherent scattering is differential interference or reinforcement of wavelengths scattered by multiple light scattering objects (x, y). Coherent scattering of specific wavelengths is dependent on the phase relationships among the scattered waves. Scattered wavelengths that are out of phase will cancel out, but scattered wavelengths that are in phase will be constructively reinforced and coherently scattered. Phase relationships of wavelengths scattered by two different objects (x, y) are given by the differences in the path lengths of light scattered by the first object (x,1–1′) and a second object (y, 2–2′) as measured from planes perpendicular to the incident and reflected waves (a, b) in the average refractive index of the media.

In summary, color produced by incoherent scattering is a function of the properties of individual scatterers (size, refractive index, shape) and the average refractive index of the medium and is independent of the phases of the scattered waves, whereas colors produced by coherent scattering are determined by the refractive index, the size *and* the spatial distribution of light scattering interfaces and are directly dependent upon the phases of the scattered waves (Fig. 1).

Incoherent scattering mechanisms include Rayleigh scattering, Tyndall scattering, and Mie scattering. Tyndall scattering refers to light scattering by small (microscopic) particles that are larger than molecules, whereas Rayleigh scattering refers to scattering by *all* small particles down to the size of individual molecules (Young, 1982). Some have argued that the because biological light scattering objects are much larger than individual molecules that Tyndall scattering

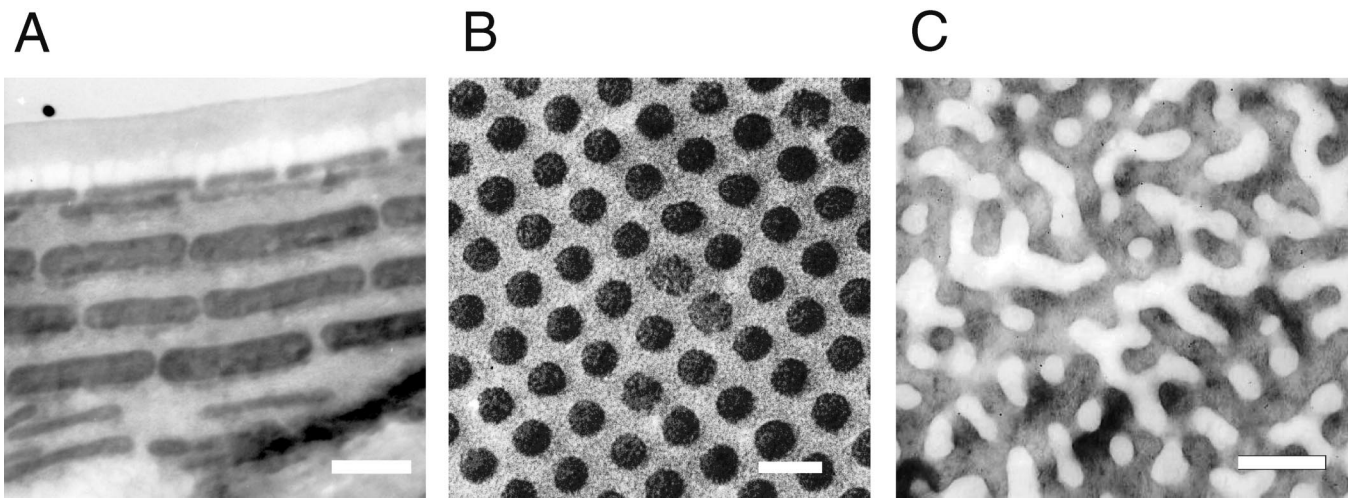

FIG. 2. Examples of the three major classes of coherently scattering nanostructures. (A) Laminar array of plate-shaped melanosomes in the barbules of the iridescent, green back feathers of the Superb Sunbird *Nectarinia coccinigastra* (Nectariniidae; TEM courtesy of Jan Dyck). Scale bar equals 200 nm. (B) Crystal-like, hexagonal array of parallel collagen fibers from the green facial caruncle of the Velvet Asity *Philepitta castanea* (Eurylaimidae; Prum *et al.*, 1994, 1999*a*). Scale bar equals 200 nm. (C) Quasi-ordered arrays of β-keratin and air vacuoles from the medullary layer of blue feather barbs of the Rose-faced Lovebird *Agapornis roseicollis* (Psittacidae; Prum *et al.*, 1999*b*). Scale bar equals 200 nm.

should be used in biological contexts (Huxley, 1975). However, since most of the explicit, testable predictions concerning small particle scattering—including the inverse relationship between scattering magnitude and the fourth power of the wavelength, and polarization—are derived from the work of Lord Rayleigh and because Rayleigh scattering includes Tyndall scattering (Young, 1982), we think is more informative to refer to biological color production by incoherent scattering from small particles as Rayleigh scattering (Prum *et al.*, 1998, 1999*a*, 2003; Prum and Torres, 2003). Mie scattering is a mathematically exact description of incoherent scattering by single particles of small or large size that simplifies to the Rayleigh scattering conditions for small particle sizes (van de Hulst, 1981; Bohren and Huffman, 1983). Examples of incoherent scattering include the blue sky, skim milk, blue smoke, and blue ice and snow.

Coherent scattering encompasses various optical phenomena that have been referred to as constructive interference, reinforcement, and diffraction. Nanostructures that coherently scatter have been referred to as thin-film reflectors, multilayer reflectors, quarter-wave stacks, Bragg scatterers, and diffraction gratings. Well known examples include the structural colors produced by brilliant iridescent butterfly wing scales and avian feather barbules, such as the peacocks tail (Dyck, 1976; Fox, 1976; Durrer, 1986; Ghiradella, 1991; Parker, 1999).

CLASSES OF COHERENTLY SCATTERING NANOSTRUCTURES

Coherent scattering typically requires spatial periodicity in refractive index. There are three, fundamental, spatial classes of coherently scattering optical nanostructures: laminar, crystal-like, and quasi-ordered.

Laminar nanostructures are composed of a series of alternating layers of two materials of different refractive indices (Fig. 2A). A single superficial layer of a distinct refractive index from the underlying substrate can also function as the simplest form of laminar optical nanostructure, like an oil slick. Laminar nanostructures include anatomical systems that have been called thin film reflectors, multilayer reflectors, and quarter-wave stacks (Huxley, 1968; Land, 1972).

Crystal-like nanostructures are composed of a square or hexagonal array of light scattering objects of a distinct refractive index from the surrounding medium (Fig. 2B). These structures are often referred to as Bragg scatterers. Color production from many superficial diffraction gratings can also be understood as coherent scattering from a crystal-like nanostructure restricted to the surface of the organism.

Quasi-ordered nanostructures are characterized by arrays of light scattering objects that are unimodal in size and interscatterer spacing, but which lack the spatial ordering at larger spatial scales (Figs. 2C, 3A). The possibility of coherent scattering by quasi-ordered nanostructures has only recently become appreciated. Dyck (1971*a*, *b*) was the first to propose explicitly that the spongy medullary keratin of structurally colored feather barbs would produce a hue by coherent scattering. However, Dyck (1971*a*, *b*) was unable to demonstrate whether the light scattering air bubbles in the spongy medullary keratin are sufficiently ordered in spatial distribution to selectively reinforce specific visible wavelengths. Benedek (1971) presented a physical explanation of how the quasi-ordered parallel collagen fibers in the vertebrate cornea are transparent to visible wavelengths despite their lack of a crystal-like lattice spatial organization. Benedek documented that the short path length additions produced by the small cor-

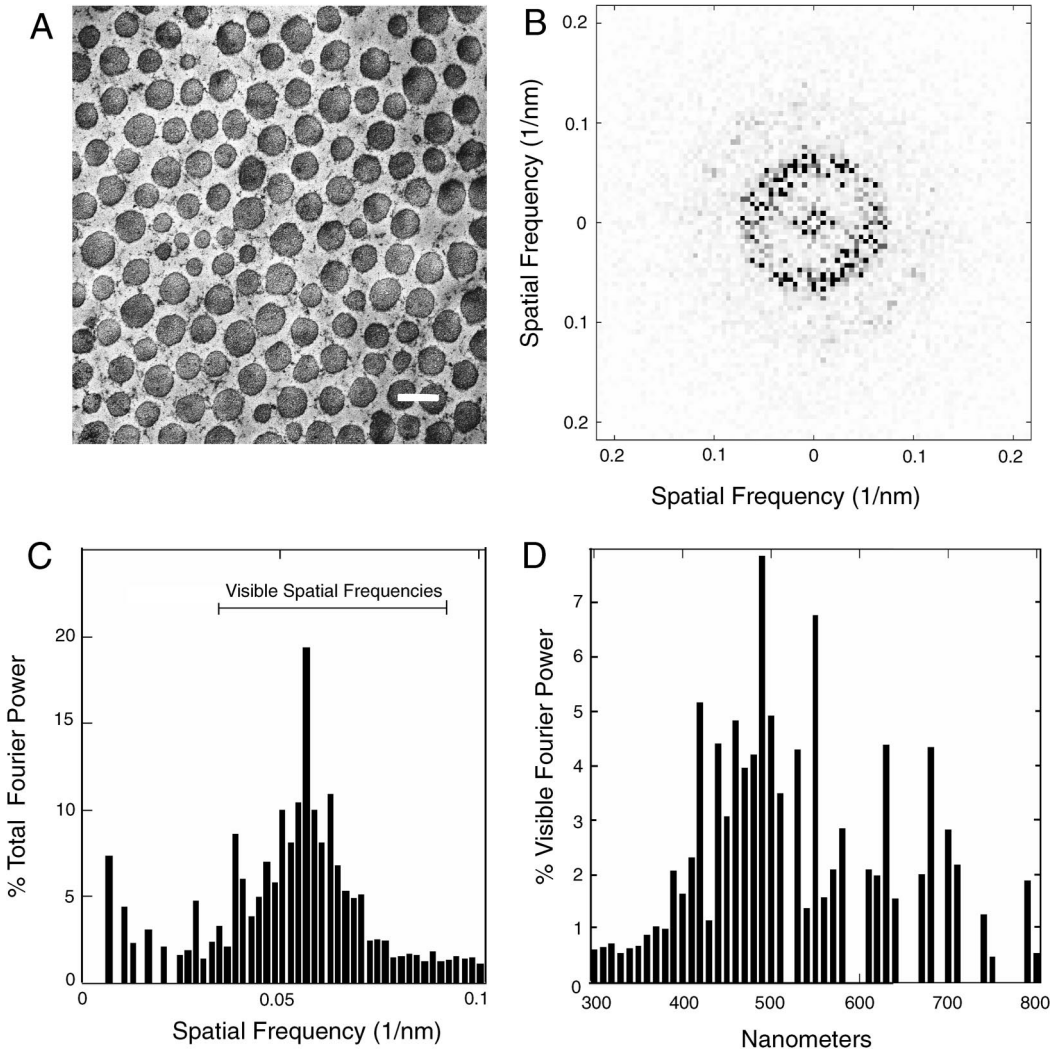

FIG. 3. Two-dimensional (2D) Fourier analysis of a quasi-ordered array of color producing dermal collagen fibers from the green throat skin of the Bare-throated Bellbird *Procnias nudicollis* (see front cover; Prum and Torres, 2003). (A) Transmission electron micrograph of the cross sections of parallel collagen fibers in the dermis. Scale bar equals 200 nm. (B) 2D Fourier power spectrum of A. Each pixel in the power spectrum depicts the relative magnitude (pixel darkness) of each component spatial frequency (distance from the origin) in all directions within the image (vector direction from the origin). The ring-shaped distribution in the power spectrum demonstrates a predominate nanoscale periodicity at intermediate spatial frequencies that is equivalent in all directions in the image. (C) Radial average of the power spectrum showing the distribution of total Fourier power among fifty uniform, radial, spatial frequency bins between O and 0.01 nm^{-1}. The overwhelming majority of the total Fourier power is distributed over spatial frequencies that are appropriate for the coherent scattering of visible light (between 0.0035 and 0.0092 nm^{-1} at an average refractive index of 1.38). D) Predicted reflectance spectrum based on the 2D Fourier power spectrum of the image, in % visible Fourier power. The power spectrum predicts a peak of coherent reflectance at 480 nm, which is closely congruent with the light green color of the tissue (see cover). This congruence indicates that the tissue is appropriately nanostructured to produce the observed hue by coherent scattering alone.

neal collagen fibers and spacing will create coherently scatter far ultraviolet light and destructively interference of all visible wavelengths yielding optical transparency. In the context of structural color production, coherent scattering is a mechanism of selective reinforcement of a subset of visible wavelengths. However, biological nano-optic structures can also exploit the same physical mechanism for the production of optical transparency. Most recently, we have experimentally demonstrated coherent scattering in the quasi-ordered spongy medullary keratin of bird feather barbs and the quasi-ordered collagen fiber arrays in avian skin (Prum *et al.*, 1998, 1999*a*, *b*, 2003; Prum and Torres, 2003).

SCATTERING AND IRIDESCENCE

Unlike incoherent scattering, coherent scattering can produce the phenomenon of iridescence—a prominent change in hue with angle of observation or illumination. Iridescence occurs when changes in the angle of observation or illumination affect the average path length of scattered waves. Changes in the distribution of path length additions to scattered waves will change the phase relationships among scattered wavelengths,

and alter which wavelengths are constructively reinforced. Strong iridescence conditions are met when the light scattering objects are arranged in laminar or crystal-like nanostructure.

In the biological literature, since at least Mason (1923*a*, *b*), iridescence has frequently been synonymized with coherent scattering (*e.g.*, Fox, 1976; Nassau, 1983; Herring, 1994; Lee, 1997). Accordingly, all iridescent structural colors were hypothesized correctly to be produced by coherent scattering, but all non-iridescent structural colors were erroneously hypothesized to be exclusively produced by incoherent scattering (Fox, 1976; Herring, 1994). The absence of iridescence was considered *prima facie* evidence of incoherent scattering.

Recently, however, it has been demonstrated that coherent light scattering by quasi-ordered arrays of light scatterers can produce biological structural colors that are non-iridescent or only weakly iridescent (Prum *et al.*, 1998, 1999*a*, *b*, 2003; Prum and Torres, 2003). Quasi-ordered arrays lack the organization at larger spatial scales that produce strong iridescence. Quasi-ordered arrays have a similar organization to a bowl of popcorn; each popped kernel is similar in size to its neighbor and center-to-center distances are quite similar, but beyond the spatial scale of a single kernel there is no organization. An example of a color producing, quasi-ordered nanostructure is the light scattering air bubbles-keratin interfaces in the layer of structurally colored avian feather barbs (Fig. 2C) (Prum *et al.*, 1998, 1999*b*, 2003); these air-keratin matrices are sufficiently spatially ordered at the appropriate nanoscale to produce the observed hues by coherent scattering but are not ordered at larger spatial scales so these colors are not iridescent, or only weakly iridescent (Osorio and Ham, 2002).

PREVIOUS METHODS OF ANALYSIS OF COHERENT SCATTERING

Most analyses of coherent scattering in biological systems have been approached from a traditional physical perspective. The most convenient or tractable mathematical solutions were used for anatomies or different classes of structures. Laminar systems have usually been analyzed with various approaches from thin-film optics (Huxley, 1968; Land, 1972; Macleod, 1986). These analyses were conducted with average or idealized measurements of laminar thickness. However, thin-film optics was recognized as being physically inappropriate for crystal-like optical nanostructures (Land, 1972). Instead, coherent scattering by crystal-like arrays have been analyzed using Bragg's Law or Bragg diffraction (Durrer, 1962; Durrer and Villiger, 1966; 1970*a*, *b*; Morris, 1975; Prum *et al.*, 1994). These applications of Bragg's Law were also based on idealized average measurements of the array dimensions.

Thin film optics and Bragg's Law have provided satisfactory analyses of structural color production by many different biological materials. In particular, matrix methods of thin film optics provide highly detailed descriptions of light coherent scattering laminar systems, including polarization, etc. (Huxley, 1968; Land, 1972; Macleod, 1986). However, neither traditional method is appropriate for the analysis of quasi-ordered arrays because quasi-ordered arrays lack the idealized lattice dimension which both methods use to calculate reflectance (Land, 1972). Both methods have additional short comings, such as their reliance on idealized average measures of array size which does not account for the inherent variation in biological nanostructures.

Traditional physical tools are mathematically incompatible with each other. Thin-film methods are based on assumptions that do not apply to crystal-like arrays. Incompatibilities among physical methods create obstacles to the analysis of the evolution of nanostructures *among* the structural classes. A simple, comparative review of the diversity of coherently scattering nanostructures in avian feather barbules indicates that many clades have apparently evolved laminar and crystal-like nanostructures from one another (unpublished data, R.O.P.).

What is required is an analytical tool that will: (1) document the spatial independence of scatters and test whether light scattering is predominantly coherent or incoherent scattering, (2) analyze coherent scattering by a biological array based on the direct observations of the spatial variation in refractive index rather than idealized average measures, and (3) analyze coherent scattering by all classes of coherently scattering nanostructural organization.

A FOURIER TOOL FOR COHERENT SCATTERING BY BIOLOGICAL NANOSTRUCTURES

In his theoretical analysis of the transparency of the vertebrate cornea, Benedek (1971) established the relationship between the Fourier transform of spatial variation in refractive index of a medium and its capacity for coherent scattering of visible light. Starting with Maxwell's equations and assuming a biological tissue composed of delta functions, Benedek (1971) concluded that those wavelengths that will be coherently scattered are equal to twice the wavelength of the predominant components of the Fourier transform of the variation in refractive index in the tissue. Subsequently, we have developed a two-dimensional (2D) Fourier analysis tool for the study of coherent light scattering by biological nanostructures (Prum *et al.*, 1998, 1999*a*, *b*, 2003; Prum and Torres, 2003).

Discrete Fourier analysis is a well known analytical tool that transforms a sample of data points into a mathematically equivalent sum of component sine waves of different frequencies and amplitudes (Briggs and Henson, 1995). The amplitudes of each of the component sine waves in the Fourier transform expresses the relative contributions of each frequency of variation to the periodicity of the original data. The plot of the variation in the squared amplitudes over all Fourier components is called the Fourier power spectrum. The relative values of the different components

in the Fourier power spectrum express the comparative contribution of those frequencies of variation to the total energy of the original function. This application of Fourier analysis is derived independently from electromagnetic optical theory (Benedek, 1971), and is independent of the traditional physical field of 'Fourier optics,' though they both describe coherence among scattered light waves.

With our nano-optic Fourier tool (available free by request from the authors), digital or digitized transmission electron micrographs (TEMs) are analyzed using the matrix algebra program MATLAB (MATLAB, 1992). The scale of each image (nm/pixel) is calculated from the number of pixels in the scale bar of the micrograph. A large, unobstructed square portion of the array is then selected for analysis. The average refractive index of each tissue is estimated by generating a two-partition histogram of image darkness (*i.e.*, the distribution of darker and lighter pixels). The frequency distribution of the darker and lighter pixels is then used to estimate the relative frequency of the two main component materials with differ in refractive index and grayscale intensity in the TEM, and to calculate a weighted average refractive index for the whole image. For accuracy, the images should have strong grayscale contrast between materials of different refractive indices.

The numerical computation of the Fourier transform is done with the well-established two-dimensional (2D) Fast Fourier Transform (FFT2) algorithm (Briggs and Henson, 1995). The Fourier transform is faster to calculate if the dimensions of the image in pixels is a power of two (*e.g.*, 512 × 512, 1024 × 1024, etc.). The Fourier transformed data are visualized with the 2D Fourier power spectrum, the distribution of the squares of the Fourier coefficients, which resolves the spatial variation in refractive index in the tissue into its periodic components in any direction from a given point (Fig. 3A–B). The 2D Fourier power spectra are expressed in spatial frequency (cycles/nm) by dividing the initial spatial frequency values by the length of the matrix (pixels in the matrix times nm/pixel). Each value in the 2D power spectrum reports the magnitude of the periodicity in the original data of a specific spatial frequency in a given direction from all points in the original image (Fig. 3B). The spatial frequency and direction of any component in the power spectrum are given by the length and direction, respectively, of a vector from the origin to that point. The magnitude is depicted by a gray scale or color scale, but the units are dimensionless values related to the total darkness of the original images.

Radial averages of the power spectra can be used to summarize the distribution of power among different spatial frequencies of variation in refractive index over all directions within an image of a tissue (Fig. 3C). This technique can be particularly appropriate for characterizing quasi-ordered arrays. Radial averages are calculated using any number of spatial frequency bins, or annuli, for a range of spatial frequency values, and are expressed in % total Fourier power. Spatial frequencies between 0 and 0.02 nm^{-1} will cover most optical phenomena. The radial averages of the power spectrum are all normalized to the total Fourier power, so a composite radial power profile can be calculated from an average of radial averages of power spectra from multiple TEM images. Also, radial averages of select quadrants, restricted slices of the power spectrum, or power profiles for single radial sections of the power spectrum can also be calculated. These alternative analyses can be highly informative for laminar and crystal-like nanostructures.

The nano-optical Fourier tool can also produce predicted reflectance spectra for coherently back scattered light based on the 2D Fourier power spectra, image scales, and average refractive indices. First, a radial average of the % power is calculated for concentric bins, or annuli, of the power spectrum corresponding to some number wavelength intervals (*e.g.*, 100 bins of 10 nm intervals) between 300 and 800 nm (covering the entire visible spectrum). The radial average power values are expressed in % visible Fourier power by normalizing the total power values across all spatial frequencies that could potentially scattering visible wavelengths (between 300 and 800 nm). The inverse of the spatial frequency averages for each wavelength are then multiplied by twice the average refractive index of the medium and expressed in terms of wavelength (nm) (Benedek, 1971). Predicted reflectance spectra can also be produced from radial analyses of a single quadrant, a custom radial slice, or a single radial section of the power spectrum. Composite predicted reflectance spectra for a tissue or sample can then be calculated by averaging the normalized predicted spectra from a sample of TEM images. The result is a theoretical prediction of the relative magnitude of coherent light scattering by the tissue, expressed in % Fourier Power, that is based entirely on the spatial variation in refractive index of the tissue.

The results of these analysis can be compared to the Fourier transforms and predicted reflectance spectra of control tissues (*e.g.*, cornea *vs.* sclera; Vaezy and Clark, 1993). However, in most cases, it is absolutely clear what nanostructures are producing the color, so it is less clear what appropriate controls might be. Further, there is no reason to expect periodicity at the appropriate nanoscale to produce visible colors other than the coherent scattering hypothesis. Power spectra of homogeneous tissues (*e.g.*, pure feather keratin) resemble white noise, whereas power spectra of highly heterogeneous material typically show an inverse frequency dependent noise (or inverse power law) distribution of Fourier components. Neither of these null distributions yields any peaks in the power spectra or predicted reflectance spectrum.

APPLICATIONS OF THE FOURIER TOOL

Rayleigh Scattering vs. Incoherent Scattering by Quasi-ordered Arrays

Prior to the invention of the electron microscope, Mason (1923*a*, *b*) firmly established the notion that

coherent scattering (*i.e.*, interference or reinforcement) is synonymous with iridescence. Because of the lack of appreciation of quasi-ordered coherently scattering nanostructures, all non-iridescent structural colors were hypothesized to be due to incoherent scattering. This hypothesis was accepted by many subsequent authors as established fact (Fox, 1976; Nassau, 1983; Herring, 1994; Lee, 1997). Following the invention of the electron microscope, observations of some hypothesized Rayleigh scattering nanostructures documented the irregular arrays that lacked the familiar laminar or crystal-like organization typical of well known interference systems (Fig. 2C). These apparently ''random'' structures were interpreted as fulfilling the predictions of the Rayleigh scattering hypothesis.

Prum *et al.* (1998) were the first to present biological structural color production in terms of the fundamental dichotomy between incoherent and light coherent scattering. Framing the question in this manner provided a new, critical test for the applicability of incoherent scattering models (including Rayleigh, Tyndall, and Mie scattering) to biological structural color production. Incoherent scattering models ignore the phases of independently scattered waves, and, thus, assume that the scatterers are randomly distributed over spatial scales of the same order of magnitude as the wavelengths of visible light (Bohren and Huffman, 1983). The 2D Fourier power spectrum of spatial variation in refractive index provides a fundamental description of the spatial periodicity of the scatterers that can test the assumption of spatial independence of scatterers required by all incoherent scattering hypotheses.

Historically, the structural colors of avian feather barbs (Häcker and Meyer, 1902; Mandoul, 1903; Tièche, 1906; Bancroft *et al.*, 1923; Mason, 1923*a*, *b*; Rawles, 1960; Lucas and Stettenheim, 1972; Fox, 1976) were long hypothesized to be produced by incoherent (Rayleigh or Tyndall) scattering. In a series of papers, we documented that the spongy air-keratin matrix of the medullary layer of structural color feathers barb rami is appropriately nanostructured to produce the observed violet, blue, green, and ultraviolet colors by coherent scattering alone (Prum *et al.*, 1998, 1999*b*, 2003). Furthermore, the ring or disk shaped peaks in the Fourier power spectra of these arrays document that the light scattering air-keratin interfaces are not spatially independent at the same spatial scale as the wavelengths visible light, falsifying the fundamental assumption of incoherent scattering.

Similarly, the blue structural colors of avian skin were long hypothesized to be produced by incoherent Rayleigh or Tyndall scattering (Mandoul, 1903; Tièche, 1906; Rawles, 1960; Lucas and Stettenheim, 1972; Fox, 1976). In an initial analysis of the Malagasy asities (Eurylaimidae, Passeriformes) (Prum *et al.*, 1999*a*, Prum and Torres, 2003) and in a subsequent survey of more than 30 species in 17 families in 10 avian orders (Prum *et al.*, 1999*a*, Prum and Torres, 2003), we have documented that the structural colors of avian skin are produced by coherent scattering from arrays of quasi-ordered parallel collagen fibers in the dermis (*e.g.*, Fig. 3A). The 2D power spectra of these tissues yield ring shaped power peaks which demonstrate substantial nanostructure at the appropriate spatial scales to produce the observed hues by coherent scattering alone (Fig. 3B).

A simple review of frequently cited instances of biological Rayleigh or Tyndall scattering documents that not one has documented the spatial independence of light scatterers (see citations in Fox, 1976; Nassau, 1983; Herring, 1994; Parker, 1999; Srinivasarao, 1999). Furthermore, the few reflectance spectra reported to match the hypothesized inverse fourth power relationship between the scattering intensity and the wavelength predicted by Rayleigh for small particle scattering are limited to a small range of visible frequencies (Dyck, 1971*a*).

Accordingly, all instances of biological structural coloration attributed to any incoherent scattering mechanism should be thoroughly and critically reevaluated (*e.g.*, Fox, 1976; Nassau, 1983; Herring, 1994; Parker, 1999; Srinivasarao, 1999). The biases in interpretation and analysis that resulted from the historical lack of appreciation of the potential for coherent scattering by quasi-ordered arrays led to the general acceptance of the role of incoherent scattering in biological color production which is completely unsupported. While it is possible that spatial independence of scatterers occurs in some anatomical systems, the previous criteria used to support a conclusion of Rayleigh or Tyndall scattering are clearly insufficient (Mason, 1923*a*; Fox, 1976).

2D Fourier analysis of a laminar array

The strongly iridescent colors of bird feathers are produced by arrays of melanin granules in the barbules of feathers (Greenewalt *et al.*, 1960; Durrer, 1962, 1986; Durrer and Villiger, 1966, 1970*a*, *b*; Dorst *et al.*, 1974; Dyck, 1976, 1987). These melanin arrays have a variety of shapes and spatial organizations, including a single keratin film, and laminar, square or hexagonal arrays of melanin granules, that have been classified into as many as 19 different types (Durrer, 1986). In previous studies, laminar and crystal-like arrays have been analyzed with either thin-film optics or Bragg's Law. However, the Fourier tool provides an additional analytical method that can provide highly accurate predictions of the shape of reflectance spectra.

Here, we present an analysis of structural color production by a laminar array from the barbules of an iridescent back feather of the Splendid Sunbird *Nectarinia coccinigastra* (Nectariniidae). Male *Nectarinia coccinigastra* have a brilliantly iridescent, deep green back with a highly saturated peak reflectance at 530 nm (Fig. 4D) (Dyck, 1976). The green hue is produced by four to six layers of flat, lozenge-shaped melanosomes separated evenly by feather keratin (Fig. 4A). The Fourier power spectra of TEMs of these laminar

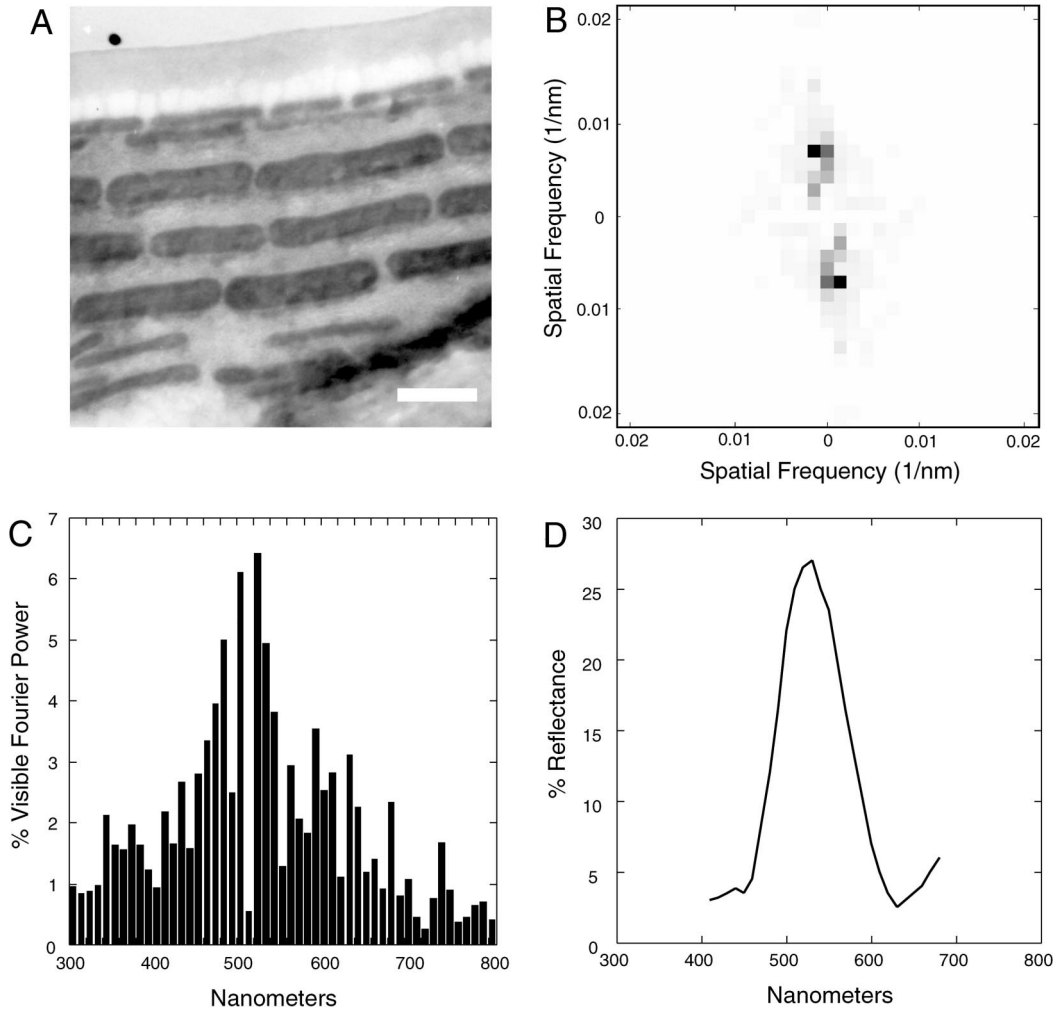

FIG. 4. 2D Fourier analysis of the laminar arrays from the Splendid Sunbird (*Nectarinia coccinigastra*, Nectariniidae). (A) Transmission electron micrographs of a laminar array of flat melanosomes from a barbule of a green back feather. Scale barb equals 200 nm. TEMs of *Nectarinia coccinigastra* are courtesy of Jan Dyck. (B) 2D Fourier power spectrum of (A). The two Fourier power peaks above and below the origin (which are displaced from vertical by the same angle as the arrays in the image) demonstrate a single predominant spatial frequency of variation in refractive index perpendicular to the layers of the array. (C) Fourier predicted reflectance spectrum based on radial averages from 27 TEM images of *Nectarinia coccinigastra*. (D) Reflectance spectrum measured from the green back feathers of *Nectarinia coccinigastra* with normal incident light from Dyck (1976).

arrays reveal a single pair of high spatial frequency peaks above and below the origin (Fig. 4B). This power spectrum indicates that the predominant Fourier components are vertically oriented waves that are perpendicular to the layers of the array. The Fourier predicted reflectance spectrum (for backscattered light with normal incident illumination) based on the average radial average from power spectra of 27 images of *Nectarinia coccinigastra* has a peak reflectance at 520 nm (Fig. 4C). The predicted reflectance is also highly saturated like the observed reflectance spectrum (Fig. 4C–D). The analysis demonstrates that the 2D Fourier method can provide accurate predictions of the peak reflectance and the shape of the reflectance spectrum for of coherent scattering by laminar arrays of 4–6 layers.

MACROEVOLUTION AMONG CLASSES OF COHERENTLY SCATTERING NANOSTRUCTURES

In the first electron microscopic examination of structurally colored avian skin, Prum *et al.* (1994) documented that the vivid structural colors of the fleshy facial caruncle of the Velvet Asity (*Philepitta castanea*, Eurylaimidae) are produced by coherent scattering by hexagonal (crystal-like) arrays of parallel dermal collagen fibers. In a subsequent comparative analysis of structural color production in *Philepitta* and its sister group, the sunbird-asities *Neodrepanis* (Prum, 1993), Prum *et al.* (1999*a*) established that the crystal-like, hexagonal nanostructure of *Philepitta* evolved from the plesiomorphic, quasi-ordered collagen nanostructure arrays like those found in *Neodrepanis*. The asities provide the first phylogenetically documented

instance of macroevolution between classes of coherently scattering, color producing nanostructures, in this case from quasi-ordered to crystal-like.

Evolution in nanostructure is necessarily accompanied by evolution in the power spectrum. Specifically, the quasi-ordered collagen arrays of *Neodrepanis* show a circular distribution of peak power, whereas the derived hexagonal arrays of *Philepitta castanea* show a hexagonal distribution of peak power values. Prum *et al.* (1999*a*) hypothesize that the hexagonal arrays of *Philepitta* evolved from the plesiomorphic quasi-ordered arrays through sexual selection for the production of a more saturated (*i.e.,* purer wavelength) hue. Accordingly, we hypothesized that female mating preferences for males with more saturated hues would correspond to selection for a narrowing of the ring of peak power values in the Fourier power spectrum. This selection would correspond anatomically to increasingly rigid specification of collagen fiber size and the distances between collagen fiber centers.

In the field of complex materials science, Torquato *et al.* (2000; Truskett *et al.,* 2000) have established two statistics for measuring spatial ordering of spheres– the translational order, or the distances between neighboring spheres; and the bond-orientation order, or the angles of vectors connecting neighboring spheres. They have documented that the two measures are positively correlated. In series of sphere packing simulations, Torquato *et al.* (2000; Truskett *et al.,* 2000) demonstrate that increases in translational order also produce increases in bond-orientation order. Analogously, the quasi-ordered nanostructure of collagen fibers of *Neodrepanis* correspond to a 2D tissue composed of circles with substantial translational order and minimal bond-orientation order. Evolution of increases in the rigidity of specification of collagen fiber distances correspond to increases in translational order, which will necessarily produce correlated increases in bond-orientation order. Thus, the 60° angles that characterize the hexagonal nanostructure of *Philepitta castanea* appear to have evolved as physical consequence of increasing nanoscale translational order.

It is easily recognized that evolution in hue among homologous structural colors can occur through small scale changes in the spatial scale of nanostructural periodicity. However, evolutionary transitions among major classes of nanostructure provide an additional dimension in which structural colors can evolve. Since different classes of nanostructure can produce additional optical properties, such as iridescence or polarization, evolution among structural classes may have major consequences for phenotype. This example of a transition from quasi-ordered to hexagonal nanostructure in the asities (Eurylaimidae) (Prum *et al.*, 1999*a*) indicates that selection on distance between light scattering objects can have a critical impact on the angles among neighboring scatterers. Why different crystal-like systems have evolved square or hexagonal arrays may have to do with the diversity of ways in which increases in translational order correspond to bond-orientation specification in different anatomical systems. Evolutionary transitions among nanostructural classes are a specific example of the more fundamental question of the initial evolution of the nanostructure from plesiomorphic anatomical structures that occurs with the first evolution of color production function. These questions should provide an important direction for future research.

PHOTONICS AND STRUCTURAL COLOR

Photonics is a new branch of physics which applies traditional methods of solid state physics and electronics to describe the interaction of photons with dielectric materials (*i.e.,* those which have periodic spatial variation in refractive index) (Joannopoulos *et al.*, 1995). These periodic dielectric materials are referred to as ''photonic crystals.'' Classical optics is based on the macroscopic description and analysis of the paths of individual light waves. In contrast, photonics focuses on analyzing which frequencies of light will be transmitted through a dielectric material. Photonics uses Maxwell's electromagnetic wave equations to analyze light in the same way that electronics applies Schrödinger's equations of quantum mechanics to analyze electrical currents (Joannopoulos *et al.*, 1995).

Since its inception (John, 1987; Yablonovitch, 1987), photonics has produced an explosion of theoretical and technological advances. One fundamental discovery has been the recognition of ''photonic band gaps''—portions of the light spectrum that cannot be transmitted or propagated through many photonic crystals (Joannopoulos *et al.*, 1995). Photonic band gaps are a product of coherent scattering, but viewed from the opposite perspective of light transmission. Since photonic crystals coherently scatter certain wavelengths, these wavelengths cannot be transmitted through these materials. Current technological research focuses on using photonic crystal material to provide cladding, or optical insulation, for fiber optics (Knight, 2003). If the photonic crystal cladding around a central fiber or space coherently back scatters certain wavelengths into the central fiber, then transmission of those wavelengths along the length of the fiber are completely insulated from escape (Knight, 2003).

Recently, biologists have begun to appreciate that color producing biological nanostructures are natural photonic crystals (Vukusic, 2003; Vukusic and Sambles, 2003), and photonic methods have been applied to a couple of exceptional biological structures (Parker *et al.*, 2001; Sundar *et al.*, 2003). But will photonic methods provide useful new perspectives and tools for understanding biological structural colors?

Photonics does provide a new and productive classification of color producing nanostructures (Joannopoulos *et al.*, 1995). Photonic crystals are classified into categories based on the number of dimensions over which there is variation in refractive index: 1D photonic crystals vary in a single dimension (*i.e.,* thin films; Figs. 2A, 4A); 2D photonic crystals vary in two dimensions, like collagen fiber arrays in bird skin

(Figs. 2B, 3A); and 3D photonic crystals have periodic variation in all three dimensions, like the spongy medullary keratin of feather barbs (Fig. 2C), or in the air-chitin matrices of many structurally colored butterfly scales (Vukusic, 2003; Vukusic and Sambles, 2003). Since photonic crystals are hypothesized to be perfectly periodic, photonics does not yet recognize the additional, biologically important distinction between outlined here between nearly perfectly periodic, crystal-like arrays and quasi-ordered arrays which have spatial periodicity limited to nearest neighbors distances (Figs. 2C, 3A). Thus, both 2D and 3D photonic crystals can be further classified as either quasi-ordered, or highly periodic and crystal-like.

From its origin in solid state physics, photonics is quite distinct from traditional optics and from those traditional optical methods applied to structural colors. Specifically, photonics methods decompose the spatial variation in refractive index of a dielectric material into its component harmonic modes, and identify which of those modes lack real solutions of Maxwell's equation (Joannopoulos *et al.*, 1995). Modes that lack real solutions constitute light frequencies that will not propagate or transmit through the material. Similarly, our Fourier method is also based on an analysis beginning with Maxwell's equations. Further, the method also decomposes the spatial variation in refractive index into harmonic components, and reconstructs predicted reflectance spectra based on the relative magnitude of those components. Thus, our Fourier tool shares with photonic theory and methods a fundamental analytical focus upon characterizing the optical consequences of periodicity of the material which is not shared by traditional optical methods.

Perfect periodicity is fundamental to photonic theory and methods. Such periodicity is common in technological materials but is extremely rare in biological nanostructures. A substantial challenge to the application of photonic methods to biological materials will be to understand deviations from perfect periodicity, especially in 2D and 3D systems. We originally developed the Fourier tool for analysis of structural color production by exactly these classes of biological materials. Further, like our Fourier tool, photonics provides a single body of methods for the analysis of a variety of structural classes of nanostructure.

In conclusion, photonic methods will likely expand available techniques for the analysis of biological structural colors. Among available methods, however, the Fourier tool is most similar to photonics in its focus on harmonic periodicity of the material and its applicability to a different classes of nanostructure.

LIMITS OF THE FOURIER TOOL

Applications of the Fourier tool are limited to analysis of structural coloration. The method does account for any potential pigmentation in the tissue, or for absorbance of light wavelengths. These limitations, however, are shared by all other available analytical tools applied to structural coloration. Additional methods are required if pigments or absorption are thought to contribute to the reflectance spectrum of an organism.

The current Fourier tool does not explicitly account for polarization, which can be substantial in nanostructures composed of highly oriented rods or particles, such as the arrays of collagen fibers. In materials with 2D periodicity in refractive index (*e.g.*, collagen fiber arrays), the reflectance spectrum predicted by the Fourier tool describes the reflectance of the transverse magnetic (TM) polarization in which the magnetic field is in the plane of the image, and the electric field is in the perpendicular plane of the fiber direction.

The current application of the Fourier tool is only suitable for 1D and 2D analyses, but we are expanding the program to apply to 3D data sets (see below).

FUTURE DIRECTIONS IN FOURIER TOOL DEVELOPMENT

We are engaged in additional development of the Fourier tool which will expand its capabilities. Primary among these is understanding the relationship between our implemented Fourier analysis and photonic methods. Also, we will be expanding the tool to analyze 3D data sets obtained by high-voltage electron microscopy or other electron tomography techniques (*e.g.*, Argyros *et al.*, 2002).

Previously, we have reported predicted reflectance spectra in terms of % visible Fourier power. Using Fresnel's equations for the efficiency of light scattering at an interface of two media of known refractive index (Huxley, 1968; Land, 1972; Hecht, 1987) and the number of objects in an array, we will be able to express the predicted reflectance spectrum in terms of % reflectance, the standard physical units of measurement.

Currently, the tool predicts reflectance of back scattered light only, and cannot decouple the angle of observation and incidence. We will implement Benedek's (Benedek, 1971) model to predicting reflectance from various angles of observation and illumination, and testing them on medullary barb keratin and other quasi-ordered nanostructures. Osorio and Ham (2002) reported significant changes in reflectance spectra from quasi-ordered medullary barb keratin by varying the angle between the incident beam and the direction of observation.

We are also developing methods to provide a statistical confidence for the match between the Fourier predicted and the independently measured reflectance spectra. By converting predicted and observed reflectance spectra to cumulative frequency distributions of total reflectance between 300–800, we can compare the fit between these cumulative distributions using the Komologorov-Smirnoff D statistic, the measure of the maximum distance between the cumulative frequency curves. By comparing D of the predicted and measured reflectance spectra to a null distribution of D values measured between the predicted spectrum and a set of null reflectance spectra of random hue and saturation, we can establish whether the match between predicted

and observed spectra are greater than would be expected by chance.

ACKNOWLEDGMENTS

Jan Dyck kindly provided micrographs of *Nectarinia coccinigastra* barbules. The development and application of the Fourier Tool have been supported by a grant to R. O. Prum and R. H. Torres from the National Science Foundation (DBI-0078376). The cover photograph of *Procnias nudicollis* is reproduced courtesy of Nate Rice.

REFERENCES

Argyros, A., M. C. J. Large, D. R. McKenzie, G. C. Cox, and D. M. Dwarte. 2002. Electron tomography and computer visualization of a three-dimensional 'photonic' crystal in a butterfly wing-scale. Micron 33:483–487.

Bancroft, W. D., E. M. Chamot, E. Merritt, and C. W. Mason. 1923. Blue feathers. Auk 40:275–300.

Benedek, G. B. 1971. Theory of transparency of the eye. Appl. Opt. 10:459–473.

Bohren, C. F. and D. R. Huffman. 1983. *Absorption and scattering of light by small particles.* John Wiley and Sons, New York.

Briggs, W. L. and V. E. Henson. 1995. *The DFT.* Society for Industrial and Applied Mathematics, Philadelphia, Pennsylvania.

Dorst, J., G. Gastaldi, R. Hagege, and J. Jacquemart. 1974. Différents aspects des barbules de quelques Paradisaeidés sur coupes en microscopie électronique. Compt. Rendu. Acad. Sci. Paris 278:285–290.

Durrer, H. 1962. Schillerfarben beim Pfau (*Pavo cristatus* L.). Verhandl. Naturf. Ges Basel 73:204–224.

Durrer, H. 1986. The skin of birds: Colouration. *In* J. Bereiter-Hahn, A. G. Matoltsky, and K. S. Richards (eds.), *Biology of the integument 2: Vertebrates,* pp. 239–247. Springer-Verlag, Berlin.

Durrer, H. and W. Villiger. 1966. Schillerfarben der Trogoniden. J. Ornithol. 107:1–26.

Durrer, H. and W. Villiger. 1970*a*. Shilleradien des Goldkuckucks. Z. Zellforschung. 109:407–413.

Durrer, H. and W. Villiger. 1970*b*. Schillerfarben der stare (*Sturnidae*). J. Ornithol. 111:133–153.

Dyck, J. 1971*a*. Structure and colour-production of the blue barbs of *Agapornis roseicollis* and *Cotinga maynana.* Z. Zellforschung. 115:17–29.

Dyck, J. 1971*b*. Structure and spectral reflectance of green and blue feathers of the Lovebird (*Agapornis roseicollis*). Biol. Skrift. (Copenhagen) 18:1–67.

Dyck, J. 1976. Structural colours. Proc. Int. Ornithol. Congr. 16: 426–437.

Dyck, J. 1987. Structure and light reflection of green feathers of fruit doves (*Ptilinopus* spp.) and an Imperial Pigeon (*Ducula concinna*). Biol. Skrift. (Copenhagen) 30:2–43.

Fox, D. L. 1976. *Animal biochromes and structural colors.* Univ. California Press, Berkeley, California.

Ghiradella, H. 1991. Light and colour on the wing: Structural colours in butterflies and moths. Appl. Opt. 30:3492–3500.

Greenewalt, C. H., W. Brandt, and D. Friel. 1960. The iridescent colors of hummingbird feathers. J. Opt. Soc. Amer. 50:1005–1013.

Häcker, V. and G. Meyer. 1902. Die blaue Farbe der Vogelfedern. Arch. Mikrosk. Anat. EntwMech 35:68–87.

Hecht, E. 1987. *Optics.* Addison-Wesley Publishing, Reading, Massachusetts.

Herring, P. J. 1994. Reflective systems in aquatic animals. Comp. Biochem. Physiol. A 109:513–546.

Huxley, A. F. 1968. A theoretical treatment of the reflexion of light by multi-layer structures. J. Exp. Biol. 48:227–245.

Huxley, J. 1975. The basis of structural colour variation in two species of *Papilio.* J. Entomol. (A) 50:9–22.

Joannopoulos, J. D., R. D. Meade, and J. N. Winn. 1995. *Photonic crystals: Molding the flow of light.* Princeton University Press, Princeton, New Jersey.

John, S. 1987. Strong localization of photons in certain disordered dielectric superlattices. Phys. Rev. Lett. 58:2486–2489.

Knight, J. C. 2003. Photonic crystal fibres. Nature 424:847–851.

Land, M. F. 1972. The physics and biology of animal reflectors. Prog. Biophys. Mol. Biol. 24:77–106.

Lee, D. W. 1991. Ultrastructural basis and function of iridescent blue colour of fruits in *Elaeocarpus.* Nature 349:260–262.

Lee, D. W. 1997. Iridescent blue plants. Am. Sci. 85:56–63.

Lucas, A. M. and P. R. Stettenheim. 1972. *Avian anatomy—integument.* U.S. Department of Agriculture Handbook, Washington, DC.

Macleod, H. A. 1986. *Thin-film optical filters.* Adam Hilger, Ltd., Bristol.

Mandoul, H. 1903. Recherches sur les colorations tègumentaires. Annales des Sciences Naturelle B. Zoologie. 8 Serie 18:225–463.

Mason, C. W. 1923*a*. Structural colors of feathers. I. J. Phys. Chem. 27:201–251.

Mason, C. W. 1923*b*. Structural colors in feathers. II. J. Phys. Chem. 27:401–447.

MATLAB. 1992. *MATLAB reference guide.* The Mathworks, Inc., Natick, Mass.

Morris, R. B. 1975. Iridescence from diffraction structures in the wing scales of *Callophrys rubi,* the Green Hairstreak. J. Entomol. (A) 49:149–152.

Nassau, K. 1983. *The physics and chemistry of color.* John Wiley & Sons, New York.

Osorio, D. and A. D. Ham. 2002. Spectral reflectance and directional properties of structural coloration in bird plumage. J. Exp. Biol. 205:2017–2027.

Parker, A. R. 1999. Invertebrate structural colours. *In* E. Savazzi (ed.), *Functional morphology of the invertebrate skeleton,* pp. 65–90. John Wiley and Sons, London.

Parker, A. R., R. C. McPhedran, D. R. McKenzie, L. C. Botten, and N.-A. P. Nicorovici. 2001. Aphrodite's Iridescence. Nature 409: 36–37.

Prum, R. O. 1993. Phylogeny, biogeography, and evolution of the broadbills (Eurylaimidae) and asities (Philepittidae) based on morphology. Auk 110:304–324.

Prum, R. O., S. Andersson, and R. H. Torres. 2003. Coherent scattering of ultravioltet light by avian feather barbs. Auk 120:163–170.

Prum, R. O., R. L. Morrison, and G. R. Ten Eyck. 1994. Structural color production by constructive reflection from ordered collagen arrays in a bird (*Philepitta castanea*: Eurylaimidae). J. Morph. 222:61–72.

Prum, R. O. and R. H. Torres. 2003. Structural colouration of avian skin: Convergent evolution of coherently scattering dermal collagen arrays. J. Exp. Biol. 206:2409–2429.

Prum, R. O., R. H. Torres, C. Kovach, S. Williamson, and S. M. Goodman. 1999*a*. Coherent light scattering by nanostructured collagen arrays in the caruncles of the Malagasy asities (Eurylaimidae: Aves). J. Exp. Biol. 202:3507–3522.

Prum, R. O., R. H. Torres, S. Williamson, and J. Dyck. 1998. Coherent light scattering by blue feather barbs. Nature 396:28–29.

Prum, R. O., R. H. Torres, S. Williamson, and J. Dyck. 1999*b*. Two-dimensional Fourier analysis of the spongy medullary keratin of structurally coloured feather barbs. Proc. R. Soc. Lond. B 266:13–22.

Rawles, M. E. 1960. The integumentary system. *In* A. J. Marshall (eds.), *Biology and comparative physiology of birds,* pp. 189–240. Academic Press, New York.

Srinivasarao, M. 1999. Nano-optics in the biological world: beetles, butterflies, birds, and moths. Chemical Reviews 99:1935–1961.

Sundar, V. C., A. D. Yablon, J. L. Grazul, M. Ilan, and J. Aizenberg. 2003. Fibre-optical features of a glass sponge. Nature 424:899–900.

Tièche, M. 1906. Über benigne Melanome (''Chromatophore'') der Haut—''blaue Naevi''. Virchows Archiv für pathologische Anatomie und Physiologie 186:216–229.

Torquato, S., T. M. Truskett, and P. G. Debenedetti. 2000. Is random

close packing of spheres well defined? Phys. Rev. Lett. 84: 2064–2067.
Truskett, T. M., S. Torquato, and P. G. Debenedetti. 2000. Towards a quantification of disorder in materials: Distinguishing disequilibrium and glassy sphere packings. Phys. Rev. E 62:993–1001.
Vaezy, S. and J. I. Clark. 1993. Quantitative analysis of the microstructure of the human cornea and sclera using 2-D Fourier methods. J. Micros. 175:93–99.
van de Hulst, H. C. 1981. *Light scattering by small particles.* Dover, New York.
Vukusic, P. 2003. Natural coatings. *In* N. Kaiser and H. K. Pulker (eds.), *2003,* pp. 1–34. Springer-Verlag, Berlin.
Vukusic, P. and J. R. Sambles. 2003. Photonic structures in biology. Nature 424:852–855.
Yablonovitch, E. 1987. Inhibited spontaneous emission in solid state physics and electronics. Phys. Rev. Lett. 58:2059–2062.
Young, A. T. 1982. Rayleigh scattering. Physics Today 35:42–48.